Materials Advances

Accepted Manuscript

This article can be cited before page numbers have been issued, to do this please use: Z. Zhou, S. Chen, Y. Shen, J. Wang, G. Zhang, Y. Shi, H. Wu, J. Luo, X. Cheng and Y. Yu, *Mater. Adv.*, 2025, DOI: 10.1039/D5MA00007F.

ROYAL SOCIETY OF CHEMISTRY

rsc.li/materials-advances

View Article Online
DOI: 10.1039/D5MA00007F

View Article Online
DOI: 10.1039/D5MA00007F

Application of a Multifunctional Liquid Crystal Material in Colorful PEDOT:PSS/Si Heterojunction Solar Cells

Zheng Zhou[abc], Shibo Chen[d], Yingming Shen[c], Juan Wang[ab], Guijun Zhang[ab],Yang Shi[ab], Haixia Wu[ab], Jingjing Luo[ab], Xiaohong Cheng*[d], Yu Yang*[ab]

[a] International Joint Research Center for Yunnan Optoelectronic Materials, School of Materials and Energy, Yunnan University, Kunming 650500, P. R. China. E-mail: yuyang@ynu.edu.cn
[b] International Joint Research Center for Optoelectronic and Energy Materials, School of Materials and Energy, Yunnan University, Kunming 650500, P. R. China. E-mail: yuyang@ynu.edu.cn
[c] Yunnan Provincial Academy of Science and Technology, Kunming 650100, P. R. China
[d] Key Laboratory of Medicinal Chemistry for Natural Resource, Ministry of Education, School of Chemical Science and Technology, Yunnan University, Kunming 650500, P. R. China. E-mail: xhcheng@ynu.edu.cn

Abstract: PEDOT:PSS/Si heterojunction solar cells (HSCs) with simple preparation process and low production costs has attracted a lot of attention. The adjustable color and good stability of devices will greatly expand their application scenarios. In this work, a liquid crystal molecule, 5,5'-bis(9-(3,4,5-tris(tetradecyloxy)benzyl)-9H-carbazol-3-yl)-2,2'-bithiophene (DT), is used as the additive and coating to fabricate colored and stable PEDOT:PSS/Si HSCs. The DT as the additive into PEDOT:PSS films can improve the conductivity of films and the junction quality of devices, leading to enhanced power conversion efficiency (PCE) of 13.24% for the uncolored devices. On based of PEDOT:PSS films adding DT, DT films with different thickness as coatings were spin-coated on the top surface of the uncolored devices, fabricating multi-color devices with the higher PCE, compared to the control devices. DT coatings can isolate air and absorb ultraviolet (UV) light, obtaining the enhanced stability for colorful devices in the air and under extreme UV irradiation. In addition, it was found that DT coatings can effectively avoid the poor uniformity of PEDOT:PSS films and disrupted linear structure of PEDOT chains under UV illumination. The work provides promising strategies for the preparation of colored and stable PEDOT:PSS/Si HSCs with high efficiency.

1. Introduction

PEDOT:PSS/Si heterojunction solar cells (HSCs) have received extensive attention due to low costs and simple solution-proceeded procedures at low-temperature.[1, 2] The colorful devices meeting the aesthetic demand of buildings are an important commercial application for PEDOT:PSS/Si HSCs. The methods of achieving color solar cells mainly include changing the color of the active layers, realizing structural color, and utilizing inkjet-printed reflective pigments, etc.[3-5] Among these methods, the achievement of structural color is a simple and practicable for obtaining color PEDOT:PSS/Si HSCs. Yang et al. fabricated vivid PEDOT:PSS/Si HSCs by controlling optical constants and thickness of PEDOT:PSS films based on the principle of optical constructive interference and destructive interference.[6] However, there is currently lack of reports about the improvement of performance and stability for colorful PEDOT:PSS/Si HSCs.

View Article Online
DOI: 10.1039/D5MA00007F

In planar PEDOT:PSS/Si HSCs, PEDOT:PSS film with main functions of charge extraction and transport is one of primary components directly determining the PCE of device.[7] Various solvents like dimethyl sulfoxide (DMSO),[8] ethylene glycol (EG)[9] or methanol (MeOH)[10] added into PEDOT:PSS solution have been adopted to increase conductivity of PEDOT:PSS film and thus augment PCE of devices.[11] And then, some materials with high conductivity or work function, such as MoO_3,[12] CoS,[13] AuNPs,[14] Au@MoS_2[7] and AgNWs[15], were mixed into PEDOT:PSS films further improving the PCE. However, a number of challenges exist for using these materials, such as expensive cost and potential toxicity.

It is widely known that the stability in operational conditions is a major issue for the commercial applications of solar cells. So far, the reported factors affecting the stability of PEDOT:PSS/Si HSCs mainly include sunlight, high temperature and moisture, which cause structural and chemical changes of the devices, and the growth of oxide layer at interface between n-Si and PEDOT:PSS.[16-18] These changes have an adverse effect on carrier separation and transport resulting in a poorer conductivity of PEDOT:PSS films and worse performance of devices. To solve these problems, an addition of dopant (dopamine,[19] waterborne acrylic resin,[20] alcohol ether solvents[21]), post-treatment (p-toluenesulfonic acid/DMSO[22]) or coverage of coating (diethyl phthalate,[23] copper iodide,[24] graphene oxide[25]) are adopted.

In addition to the above-mentioned factors, Santonicola and Cremades group found that ultraviolet irradiation can change the molecular arrangement of PEDOT and decrease the conductivity of film, significantly affecting the photoelectric performance of device.[26, 27] However, how to reduce the impact of UV on stability has not yet been effectively addressed. Hence, a new effective method is needed to comprehensively solve the multifaceted stability issues, especially for UV illumination. According to the above discussion, in order to enhance the potential of PEDOT:PSS/Si HSCs application, it is critical to improve efficiency, enhance stability and adjust color of the device. However, simultaneous addressing of these three challenges, especially using only one material, has been rarely investigated.

In this paper, we propose a low cost, low temperature and solution-proceeded method to fabricate PEDOT:PSS/Si HSCs by using a liquid crystal molecule, namely 5,5'-bis(9-(3,4,5-tris(tetradecyloxy)benzyl)-9H-carbazol-3-yl)-2,2'-bithiophene (DT), as an additive and coating which realize color tuning, better stability and higher efficiency. The DT have three main functions: (i) The DT is introduced into PEDOT:PSS to achieve highly efficient devices. After adding DT, the changes of structure and surface topography for PEDOT:PSS films can effectively enhance conductivity, thus strongly reducing leakage current efficiency, promoting good junction quality and lowering series resistance in DT modified devices. Consequently, the device achieves a higher PCE of 13.24% after adding DT than that of reference device without DT. (ii) The DT coatings were spin-coated on the external surface of devices with adding DT, the colored devices with different hue were made by adjusting the combined thickness of PEDOT:PSS film and DT coating. The champion PCE of the colored devices is 12.23%, which is higher than that of the uncolored reference devices without DT coating. (iii) The DT films of colored devices were served as protective layer, which not only isolate moisture in air but also absorb UV radiation, significantly raising stability of devices especially anti-ultraviolet capability. The device covered by DT coating retains 84% of initial PCE after 11 hours under strong illumination by UV lamp, compared with 36% for the device uncovered by DT coating.

2. Experimental

View Article Online
DOI: 10.1039/D5MA00007F

2.1. Materials and PEDOT:PSS solutions preparation

Dimethyl sulfoxide (DMSO, 99.9%, Aladdin), tetrahydrofuran (THF, 99.9%, Aladdin), Triton X-100 (Sigma–Aldrich), PEDOT:PSS (Clevis PH1000, Heraeus) and n-Si (resistivity 0.05–0.1 Ω cm, orientation <100>, one-side polished, the thickness of 300 μm, Suzhou Research Materials Microtech Co., LTD) were purchased. DT liquid crystal powder was synthesized as previously published.[28] Firstly, the PEDOT:PSS solution was mixed with 5 wt% DMSO and 0.2 wt% Triton-100 and then was stirred for 6−8 h. Next, the DT powder was dispersed in THF with different concentrations (0.8, 1.0, 1.1, 1.2, 1.3, 1.4, 5, 10 mg mL^{-1}). Finally, PEDOT:PSS solution and 1 vol % DT solution with different concentrations were mixed, stirred and ultrasonically dispersed to form the precursor solution.

2.2 PEDOT:PSS/Si HSCs Fabrication

Fig. 1 shows the preparation process of planar colored PEDOT:PSS/Si HSCs. One-side polished n-type Si wafers were cleaned with a standard RCA procedure. Firstly, the different precursor PEDOT:PSS solution was spin-coated on the Si substrates and annealed at 130 °C for 30 min. PEDOT:PSS films or one with an addition of DT (PEDOT:PSS+DT films) were obtained. Then, the Ag-grid front electrode with thickness 200 nm (9% coverage of the device surface) and Al rear electrode with thickness 80 nm were thermally evaporated on the rear and front sides of devices, and then uncolored devices were fabricated. Secondly, to tune the hue of samples, we deposited DT films of moderate thickness on the top surface of uncolored devices by using a spin-coating procedure. The different thickness of DT films were obtained by spin-coating various concentration of DT solution at different spin-coating rate.

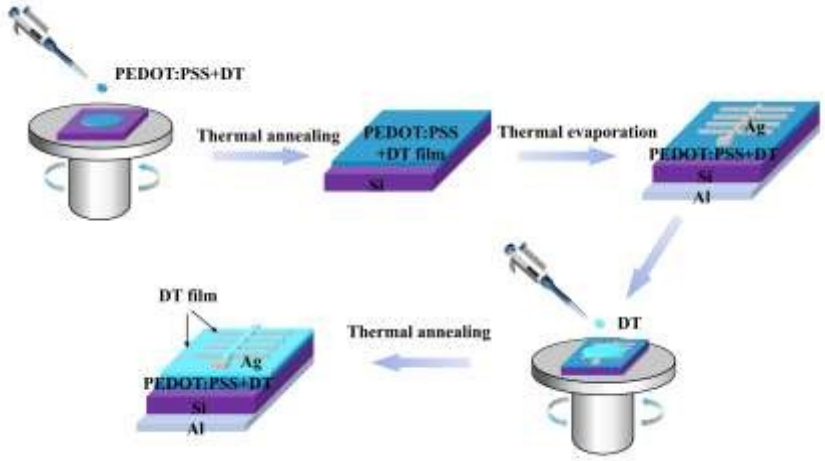

Figure.1 The schematic diagram of fabrication process of colored devices.

2.3 characterization

Atomic force microscopy (AFM, Bruker MultiMode 8) was used to analyze the surface morphology of the PEDOT:PSS films on Si wafer. UV−visible transmittance spectra of the PEDOT:PSS films on glass were measured with a spectrophotometer (UV-3600). The Raman spectrum of the PEDOT:PSS films on Si wafer were measured by Raman microscopy (inVia, Renishaw). The XPS characterization of the PEDOT:PSS films on Si wafer was performed by

View Article Online
DOI: 10.1039/D5MA00007F

using a X-ray photoelectron spectrometer (XPS, Thermo Fisher Scientific, K-Alpha+). The electrical properties of PEDOT:PSS films on the glass was tested by the Hall measurement system (East Changing, HT-100). The thickness of PEDOT:PSS films and DT coatings on Si wafer was measured by DektakXTL (Bruker). The photovoltaic performance of devices was measured under Air-mass 1.5 illumination (100 mW cm^{-2}) or dark condition by using Keithley 2400. During the measurements of photovoltaic parameters of devices coated DT films, DT films coverd on the square electrode of Ag-grid were erased with THF to allow the test probe to directly contact the square electrode of silver grid. All of devices were shielded with an opaque mask with an designated open area of 0.72 cm^2, allowing light to illuminate the devices.

3. Results and Discussion

3.1. Characteristics and functions of DT

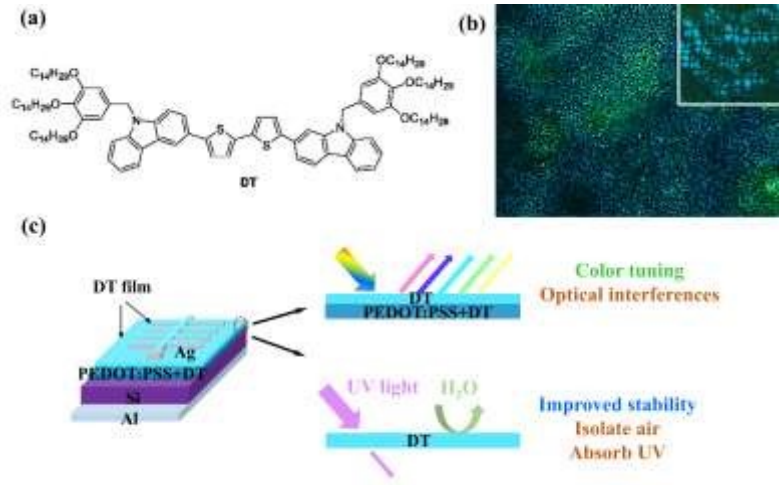

Figure 2. (a) The chemical structure of DT. (b) The image of DT by polarized optical microscopy. (c) The schematic diagram of two functions of DT coating for colorful and stable devices.

The DT is a compound with superior semiconductive property and remarkable self-assembly reported by Chen.[28] Fig. 2a shows the molecular structure of DT. To investigate the liquid-crystalline behavior of DT molecule, it was cooled down from isotropic states at 115° C to room temperature and observed by using polarized optical microscopy (POM). As shown in Fig. 2b, there is orderly and continuously spherulitic fanlike textures with hexagonal columnar phase for DT molecule, which can form not only uniform film with good crystallinity, but also a carrier transport channel with excellent charge transport capability.[28-31]

In addition, it was reported by Chen that DT films exhibit an absorption maximum at 399 nm and mainly absorbs light with wavelengths below 450nm.[28] As shown in Fig. S1, DT films have a transmittance exceeding 98% and almost are transparent for most of incident light above 450nm which is the main wavelength range absorbed by devices, whereas similar to the literature, there is obvious absorption for the DT films below 450nm, suggesting that DT films can effectively prevent UV light from reaching the PEDOT:PSS film. According to results and analysis above mentioned, the DT is expected to have the great potential as the addictive and coating to fabricate colored and stable devices. When DT films were used as coatings covered on uncolored devices, the configuration of devices is shown in Fig. 2c. Meanwhile Fig. 2c also shows two functions of DT coatings: (1) based on the principle of light interference effects between the DT film and PEDOT:PSS film, as reported in previous papers by Yang and Jiang groups,[6, 32] colorful devices with configurations of Al/Si/PEDOT:PSS/Ag/DT (colored control device) or

Al/Si/PEDOT:PSS+DT/Ag/DT (colored DT-added device) were fabricated. (2) The DT coating on the outer surface of devices can be served as an encapsulation layer to block moisture from the air and especially a protective layer to reduce the damage of UV light to PEDOT: PSS films, further improving the stability of devices in the air and under UV radiation. And detailed effects of DT on the photovoltaic performance, color control, and stability improvement of devices will be discussed and evaluated thoroughly in next section.

3.2. Effect of DT on PEDOT:PSS film

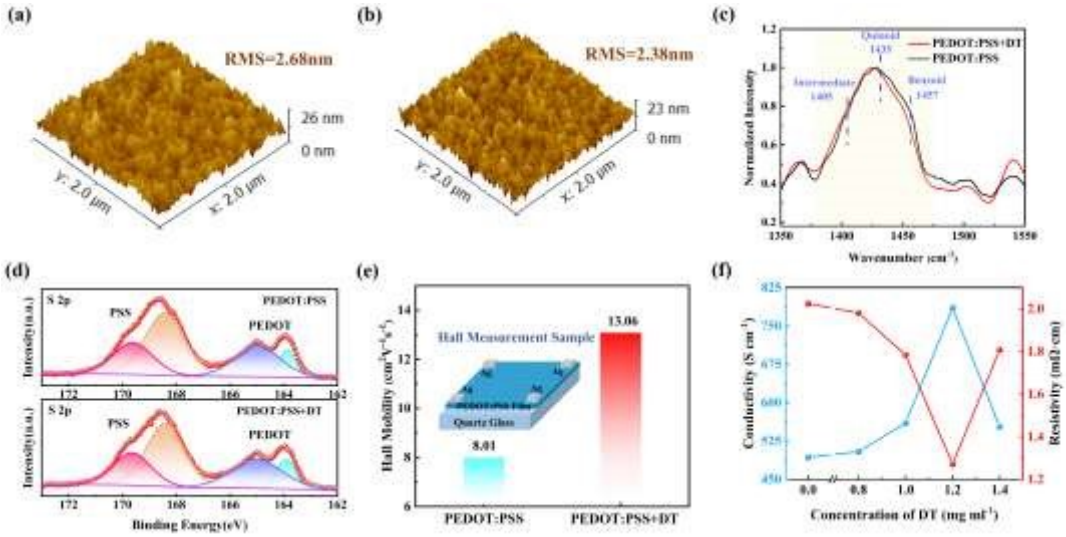

Figure 3. Root means square roughness images of the (a) PEDOT:PSS films and (b) PEDOT:PSS+DT films. (c) Normalized Raman spectrum, (d) XPS spectra in the S 2p regions and (e) Hall mobility by Hall measurement of PEDOT:PSS film and PEDOT:PSS+DT films. (f) Conductivity and resistivity of PEDOT:PSS films with the addition of different concentrations of DT solution.

To investigate the impact of DT additive on PEDOT:PSS films, we fabricated and characterized PEDOT:PSS films and PEDOT:PSS+DT films. The POM was used to explore the crystalline state of PEDOT:PSS films. As shown in Fig. S2, the POM images show that PEDOT:PSS+DT films contain liquid crystal phase compared to PEDOT:PSS film, illustrating that DT was successfully introduced into PEDOT:PSS film. The AFM characterization was conducted to study the surface morphology, which is very important for achieving high conductivity of PEDOT:PSS films. In the AFM morphology and phase images (Fig. S3a–d), the brighter regions and darker regions can be assigned to PEDOT and PSS respectively.[9, 33] There are both good interconnection of PEDOT chains consisted of fine fiber-like structures for PEDOT:PSS films with or without DT. However, RMS reduced from 2.68 nm of PEDOT:PSS film to 2.38 nm of PEDOT:PSS+DT film in Fig. 3a-b. The results of AFM show that the PEDOT:PSS film adding an appropriate amount of DT not only maintain good linear structure of PEDOT:PSS being beneficial to excellent charge transfer, but also present good crystallinity and improve the surface uniformity meeting application requirements of planar devices.[34, 35]

To investigate structural change of PEDOT:PSS films, Raman spectra and XPS were carried out. For the stretching vibration of the Cα=Cβ of the five-member thiophene ring of PEDOT:PSS at the band around 1430 cm^{-1} in Raman spectra (Fig. 3c), there are three peaks containing 1405 cm^{-1} of benzoid symmetric stretching, 1435 cm^{-1} of quinoid symmetric stretching and 1457 cm^{-1} of an intermediate state absorption modes.[9, 36, 37] The position peak of the starching vibration of

View Article Online
DOI: 10.1039/D5MA00007F

Cα=Cβ band appears an slightly redshift from 1428 cm^{-1} to 1424 cm^{-1} after DT addition, demonstrating that PEDOT chains change from a coil structure to an extended-coil or linear structure.[23] Moreover, after the DT addition, the peak of the benzoid structure shows a decreasing trend, whereas one of the intermediate state presents a slightly increasing trend, indicating that the structure of PEDOT chains change from benzoid structure with lower conductivity to an intermediate state with higher conductivity. These structure changes are beneficial to increase the conductivity of PEDOT:PSS films.[38] As shown in Fig. S4, the binding energy of 162–167 eV corresponds to thiophene rings of PEDOT and that of 167–172 eV attributes to sulfonate groups of PSS in XPS spectrum of S 2p.[39] It can be seen that the PEDOT/PSS ratio has grown. To obtain the more accurate PEDOT/PSS ratio, the quantified PEDOT/PSS ratios were calculated from Fig. 3d. After adding DT, the PEDOT/PSS ratio increased from 0.48 to 0.56, which indicating that more insulate PSS and conductive PEDOT were separated resulting in the higher conductivity for PEDOT:PSS+DT films.[40]

On the basis of the above analysis about spherulitic fanlike textures of DT and changes of the morphology and structure of PEDOT:PSS films, the Hall measurement was conducted to study the charge transport of PEDOT:PSS films without or with DT. Corresponding Hall mobility and Hall sample structure are exhibited in Fig. 3e. After adding DT, the Hall mobility increases from 8.01 $cm^2\ V^{-1}\ s^{-1}$ of PEDOT:PSS film to 13.06 $cm^2\ V^{-1}\ s^{-1}$ of PEDOT:PSS+DT film, which demonstrates that the improved carriers transport properties was effectively achieved. Moreover, the electrical conductivity of different PEDOT:PSS films are showed in Fig. 3f. As adding DT concentrations from 0 to 1.4 mg ml^{-1}, the conductivity of PEDOT:PSS films firstly increase and then decrease, whereas the resistivity shows an adverse trend. With an addition of proper concentration of DT at 1.2 mg ml^{-1}, the resistivity of PEDOT:PSS+DT film can be decreased from 2.02 to 1.27 mΩ cm, while the highest conductivity of 785 S cm^{-1} was obtained and obviously higher than that of PEDOT:PSS film. The enhanced carriers transport capability will result in an improved photovoltaic performance of devices.

3.3. Photovoltaic performance of devices

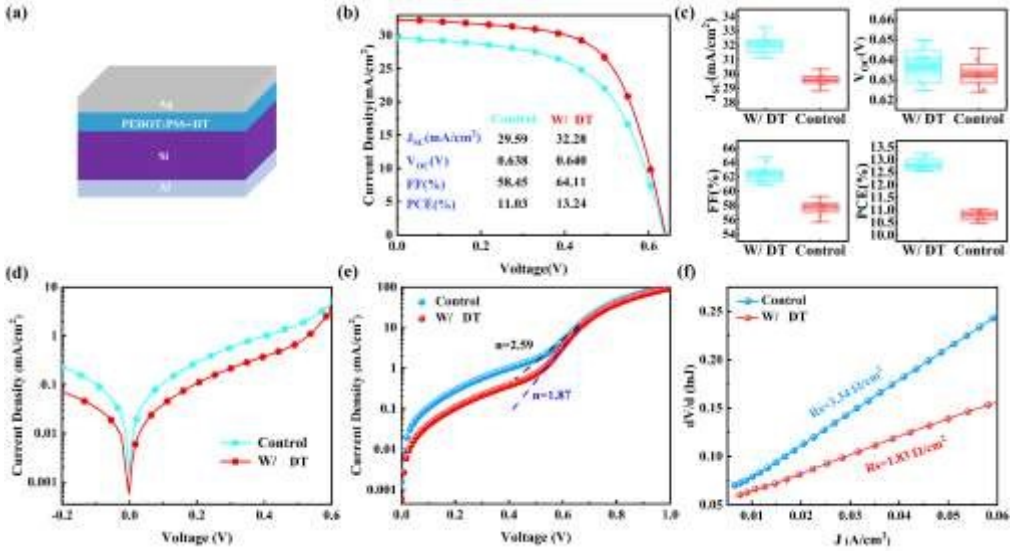

Figure 4. (a) The schematic diagram of devices with DT. (b) The light current J–V curves, (c) statistical plots of photovoltaic performance and (d) dark J–V curves of devices with or without DT. (e) Linear fitting and (f) dV/d(lnJ)–J curves calculated from dark J–V curves of devices without and with DT.

To analyze the effect of PEDOT:PSS+DT films on the photovoltaic performance, the planar devices (Fig. 4a) with the architecture of Al/Si/PEDOT:PSS+DT/Ag were fabricated, while ones with the architecture of Al/Si/PEDOT:PSS/Ag were used as control device. The current density–voltage (J–V) curves of devices under illumination, and the related photoelectric parameters including the short–circuit current density (J_{SC}), open–circuit voltage (V_{OC}), filling factor (FF) and PCE are displayed in Fig. 4b. The PCE of control device was 11.03% with a J_{SC} of 29.59 mA cm^{-2}, V_{OC} of 0.638 V, and FF of 58.45% respectively. Interestingly, for the DT-added devices, an improved champion PCE of 13.24% was achieved with a J_{SC} of 32.28 mA cm^{-2}, V_{OC} of 0.640 V, and FF of 64.11%. The J–V curves of devices with different concentrations of DT are shown in Fig. S5, and the corresponding parameters are displayed in Table S1, respectively. As shown in statistical plots of photovoltaic parameters (Fig. 4c), it is worth noting that main factors of the improved PCE were the enhancement of J_{SC} and FF.

To explain the reason for the increase of photovoltaic characteristics, the J–V curves of the corresponding devices under dark conditions were measured. It can be seen that the DT–added device had a reduced leakage current in Fig. 4d, indicating better charge extraction and collection efficiency and thus is beneficial for the enhancement of Jsc and FF.[7, 40] The dark J–V curves of devices with different concentrations of DT are shown in Fig. S6. The ideal factor (n) and reverse saturation current density (J_0) were calculated from the following formula:

$$J_{\text{dark}}(V) = J_0\left[\exp\left(\frac{eV}{nkT}\right)-1\right]$$

where J_{dark} is the current density value, V is the applied voltage, T is the absolute temperature, k is the Boltzmann constant, and e is the electronic charge.[41] As shown in Fig. 4e, the n decreased from 2.59 of the control device to 1.87 of DT–added device demonstrating the improved junction quality of the PEDOT:PSS/Si interface, enhanced rectifying characteristics and less recombination of devices after adding DT. Meanwhile, it can be seen that J_0 dropped by several orders of magnitude from 5.73×10^{-4} A cm^{-2} of control device to 8.04×10^{-6} A cm^{-2} of DT–added device leading to the lower leakage current and the higher J_{SC}. The series resistance (R_S) was also extracted from the dark J–V curves and has an important impact on the FF of devices, namely a smaller R_S will result in a higher FF than the larger one.[41-43] As shown in Fig. 4f, the control device had a larger R_S of 3.34 Ω cm^2, and the Rs dropped to 1.83 Ω cm^2 for DT–added devices. For devices with different DT concentration, the change of Rs and FF presented an opposite trend in Fig. S7. In fact, after an addition of DT, the decreasing value of Rs is also attributed to upgrading junction quality and increasing conductivity. All the optimization of the n, J_0 and R_S of DT–added devices can be conducive to the enhancement of FF and Jsc.[7] Besides, the increase of conductivity and decrease of resistivity for PEDOT:PSS+DT films with a moderate addition of DT discussed above are important factors as well leading to accelerating charge transportation and less recombination losses, which has more contribution to the Jsc and FF.[44]

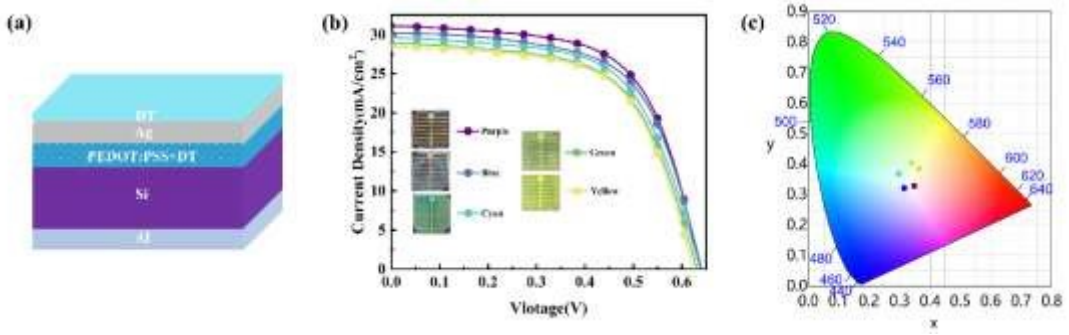

View Article Online
DOI: 10.1039/D5MA00007F

Figure 5. (a) The schematic diagram of colored devices. (b) The light current J–V curves of colorful devices. (c) The Coordinates of colored devices in the CIE 1931 chromaticity diagram.

Fig. 5a shows the structure of the colored devices. To adjust the hue of devices, different thickness of DT coating were covered on the top surface of DT-added devices with the thickness of PEDOT:PSS+DT films or PEDOT:PSS films fixed around 100nm. As shown in Fig. S8, the champion PCE of the control device is 11.03% with a J_{SC} of 29.59 mA cm^{-2}, whereas that of colored control devices (reference purple devices) dropped to 10.44% with a J_{SC} of 28.57 mA cm^{-2}. The Jsc and PCE of the colored device obviously decreased, as the DT coating increases reflection and diminishes absorption of incident light. To enhance the photovoltaic performance of colored devices, DT as additive is also introduced into PEDOT:PSS film, and then more efficient colorful DT-added devices were obtained. The graph and J–V curves of colored sample with PEDOT:PSS+DT films are shown in Fig. 5b and the relate CIE 1931 chromaticity diagram are presented in Fig. 5c. It can be seen that the purple, blue, cyan, green and yellow devices were obtained corresponding CIE 1931 color coordinates, thickness and photoelectric parameters presented in Table 1. Noticeably, the photovoltaic performance of the purple device with adding DT was obviously enhanced compared to the reference purple device. It had the thinnest thickness of DT coating and lowest optical loss yielding the highest J_{SC} of 29.29 mA cm^{-2} and PCE of 12.36%. Moreover, there are slight difference in Voc and FF for colorful devices, whereas the J_{SC} of 28.40–31.13 mA cm^{-2} and PCE of 10.94–12.36% from purple to yellow shows a significant decline as DT film thickness increasing. Very interestingly, although the champion PCE of color devices are lower than that (13.24%) of the dark-color DT-added device without coating, it is higher than that (11.03%) of the control device without adding DT and DT coating. In addition, all colorful devices have a relative PCE of over 99% compared to uncolored control devices. These results demonstrate that such method for obtaining vivid solar cells is practicable and potential for broadening novel applications.

Table 2

Device parameters of colored devices with DT coating.

Colored devices	Thickness of PEDOT:PSS+DT and DT film (nm)	CIE 1931 (x, y)	J_{SC} (mA cm^{-2})	V_{OC} (mV)	FF (%)	PCE (%)
Purple	110	(0.3466, 0.3279)	31.13	0.638	62.25	12.36
Blue	120	(0.3154, 0.3213)	30.26	0.641	61.51	11.92
Cyan	160	(0.2982, 0.3682)	29.65	0.638	60.90	11.52
Green	370	(0.3405, 0.4046)	28.89	0.631	60.58	11.04
Yellow	220	(0.3642, 0.3854)	28.40	0.623	61.82	10.94

3.4 The stability of devices

View Article Online
DOI: 10.1039/D5MA00007F

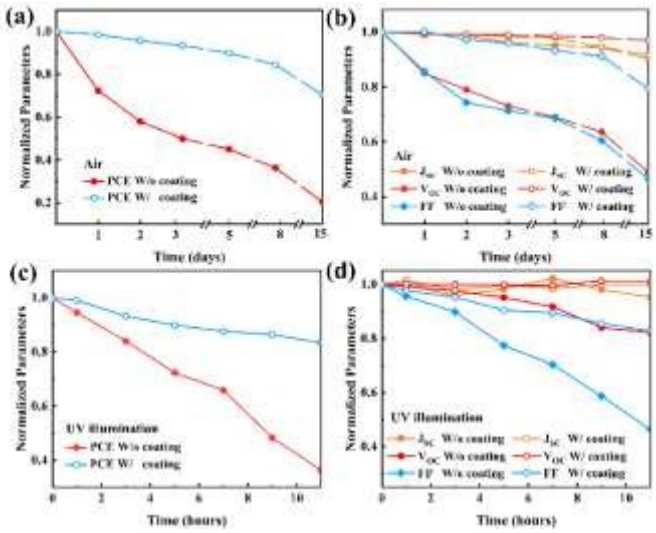

Figure 6. (a) Normalized PCE and (b) photovoltaic parameters degradation of the devices in the air. (c) Normalized PCE and (d) photovoltaic parameters degradation of the devices in the air and under UV illumination.

The a good stability is very critical for enhancing the possibility of commercial applications for PEDOT:PSS/Si HSCs. As shown in Fig. 6a–b, there is a slower deterioration in V_{OC}, FF and PCE for the colored devices covered by DT coating compared to the control device uncovered by DT coating in air at room temperature and relative humidity of 60%. The colored devices retains 70% of its initial PCE after 15 days, while the control device only maintains 20%, suggesting that DT coating can act as an encapsulating layer of the devices to obtain the better stability in the air, as DT films are able to effectively avoid the moisture absorption of PEDOT:PSS.[23] In addition, the extreme aging tests for the devices were conducted by keeping devices directly to be irradiate by UV lamp in ambient atmosphere at room temperature and relative humidity of 60%. As shown in Fig. S9, under UV irradiation, devices covered with DT coating can absorb UV and emit green light, while those without DT coverage did not emit light. Fig. 6c-d show the PCE and FF of devices without DT coating quickly drops to 36% and 46% respectively under strong UV illumination and in ambient atmosphere for 11 hours, whereas the PCE and FF of devices without DT coating kept only in ambient atmosphere for 1 days just reduced to 72% and 85% in Fig 4a-b. This finding shows that UV light can further accelerate the degradation rate of photovoltaic performance of the devices, on the basis of the degradation of stability caused by ambient atmosphere. Interestingly, the device covered by DT coating exhibits only 16% PCE degradation under intense UV radiation for 11 hours, while the PCE degradation of control device is higher by 64%. Meanwhile, after UV exposure, the device covered by DT coating shows slower decline trends with the V_{OC} and FF compared to the device uncovered by DT coating. These results demonstrate that DT-coated devices have superiority in stability due to UV absorption of DT films.

View Article Online
DOI: 10.1039/D5MA00007F

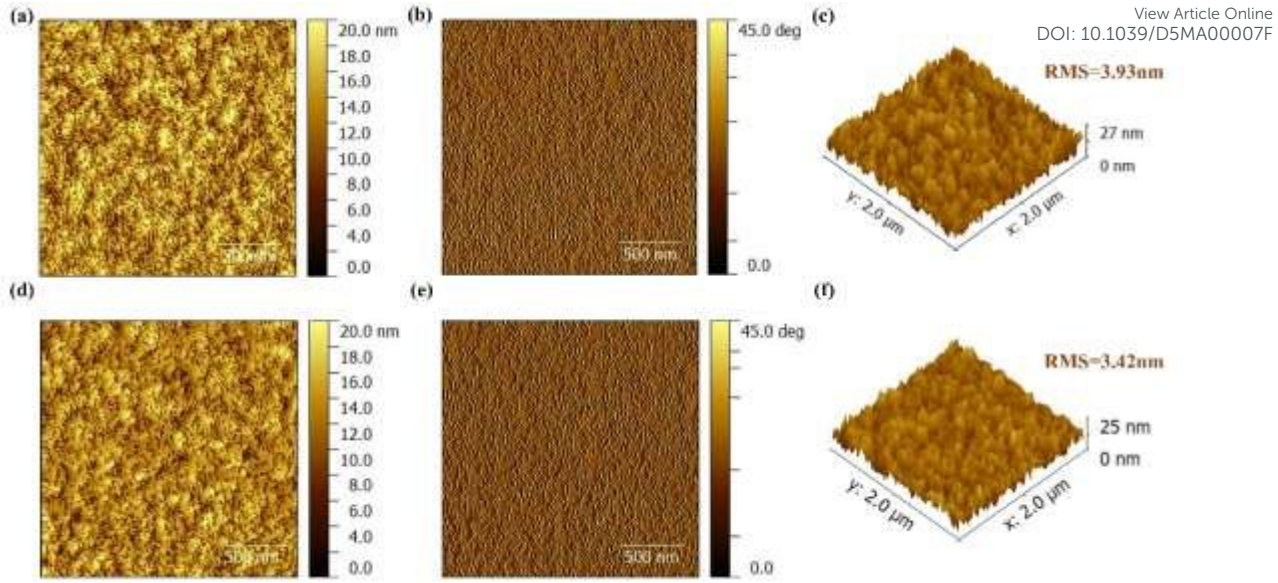

Figure 7. (a) AFM morphology, (b) phase images and (c) RMS of the PEDOT:PSS film under UV illumination. (d) AFM morphology, (e) phase images and (f) RMS of the PEDOT:PSS film with DT coating under UV illumination.

To investigate the influence of UV radiation on stability, PEDOT:PSS films were kept under UV lamp in the glove box for 11 hours. The AFM measurements shows a significant changes of morphology, phase and RMS for the PEDOT:PSS film after UV illumination. Compared to Fig. S2a-b, the morphology and phase images in Fig. 7a-b show that the better fiber-like interconnection of conductive PEDOT chains were broken and an apparently clustered PEDOT were randomly surrounded by PSS for PEDOT:PSS film illuminated by UV. Moreover, the RMS significantly raised from 2.68 nm (Fig. 3a) to 3.93 nm (Fig. 7c) with a nearly 50% growth rate, suggesting the worse continuity of PEDOT:PSS film after UV illumination. As shown in Fig. 7d-f, although PEDOT chains were also damaged after UV irradiation, PEDOT:PSS film with DT coating still maintained a better linear structure of PEDOT less surrounded by PSS and exhibited a lower RMS (3.42 nm) than that without DT coating. The results demonstrated that the DT coating can reduce the damage to morphology of PEDOT:PSS films caused by UV irradiation.

View Article Online
DOI: 10.1039/D5MA00007F

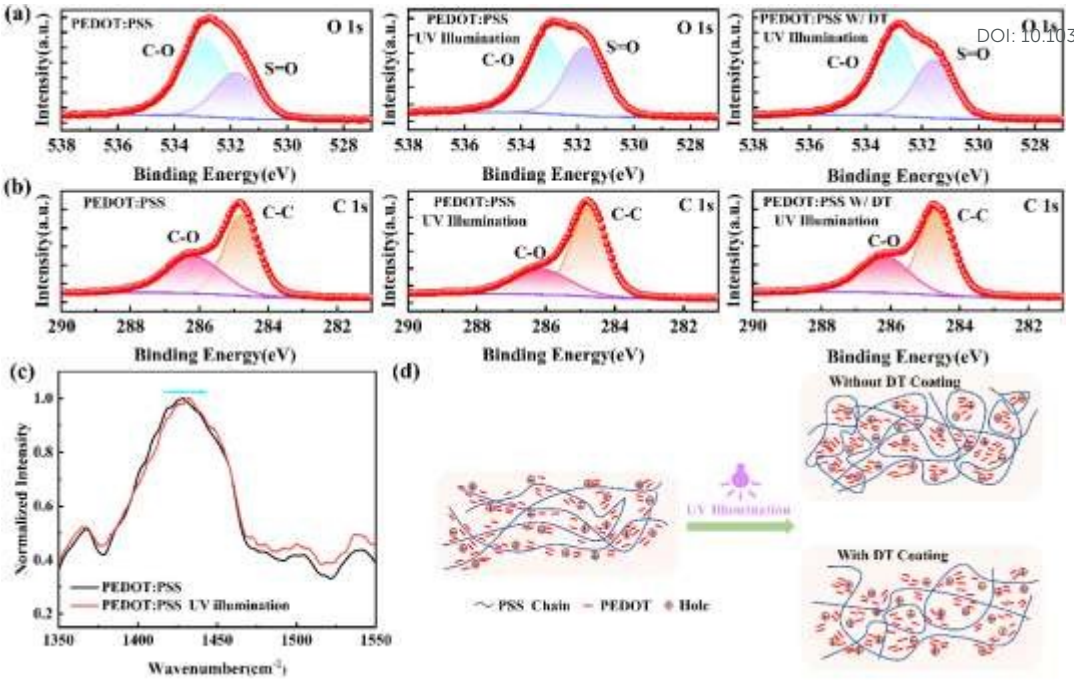

Figure 8. The XPS spectra in the (a) O 1s and (b) C 1s regions of the fresh as-prepared PEDOT:PSS film, PEDOT:PSS film without and with DT coating illuminated by UV lamp. (c) The Normalized Raman spectrum of the fresh as-prepared PEDOT:PSS film and PEDOT:PSS film illuminated by UV lamp. (d) The schematic diagram of the change of PEDOT:PSS film with or without DT coating after UV illumination.

Fig. 8a-b show the C1s and O1s XPS spectra of fresh as-prepared PEDOT:PSS film and one with or without DT coating illuminated by UV lamp. For the O 1s spectra, there are two peaks containing the C–O of PEDOT at 533 eV and S=O of PSS at 531 eV. [45] After UV illumination, the O1s peak area ratio between PSS and PEDOT increased in Fig. 8a, indicating that the C–O structures in PEDOT has reduced, while the peak value of C-O of PEDOT at 286.2 eV in C1s XPS band (Fig. 8b) also decreased further demonstrating the breaking of C–O bonds in PEDOT.[46] These changes of C–O structures confirmed that the conjugated structure of PEDOT was disrupted.[23] Meanwhile, it can be seen from Fig. 8a-b that there was the less cleavage of C–O bonds in PEDOT for PEDOT:PSS films covered by DT coating. To further analyze the structure of PEDOT after UV illumination, the result of the Raman spectrum is conducted in Fig. 8c. The Raman spectrum of the fresh as-prepared PEDOT:PSS film presents a main peak at 1426 cm^{-1}. However, the blue shift to 1435 cm^{-1} was be observed after UV irradiation, which indicating a increasing coiled conformation and cluster of PEDOT groups in PEDOT:PSS films.[47, 48]

Based on the above analysis about AFM, XPS and Raman spectrum, the effect of UV irradiation on PEDOT:PSS films was exhibited schematically in Fig. 8d. For the PEDOT:PSS films after UV irradiation, the disrupted linear structure of PEDOT damaged the charge transfer channel, while the conductive PEDOT more tightly surrounded by insulating PSS limiting the charge transfer and hopping. These adverse changes caused a decrease in the conductivity of the PEDOT:PSS films leading to the worse stability of devices. However, for PEDOT: PSS films covered by DT coating, the negative impact of UV illumination on PEDOT: PSS films is relatively weak, namely there are less disrupted structure and morphology. The results illustrate that DT coating can effectively enhance the stability of structure and morphology of PEDOT:PSS films, thus leading to improved stability of the DT-coated color devices under UV illumination.

Table 3

View Article Online
DOI: 10.1039/D5MA00007F

Comparison of various materials as the additive of PEDOT:PSS films or the coating of devices for planar PEDOT:PSS/Si HSCs.

Material	Role in devices	Method	Device structure	Device color	Stability	Improved PCE	Ref.
DT	Additive Coating	Spin-coating	Uncolored device: Al/Si/PEDOT:PSS+ DT/Ag Colored device: Al/Si/PEDOT:PSS+ DT/Ag/DT	Multi-color	Enhanced stability in the air and under extreme UV irradiation	Uncolored device: 13.24% Colored device: 12.36%	Our Work
Vanadium Pentoxide (V_2O_5)	Additive	Spin-coating	Al/Si/PEDOT:PSS+ V_2O_5/Ag	Dark	-	15.17%	40
WA	Additive	Spin-coating	Al/Si/PEDOT:PSS+ WA/Ag	Dark	Enhanced stability in the air and under extreme UV irradiation	13.37%	20
2,3,5,6-tetrafluoro-7,7,8,8-tetracyanoquinodimethane (F4TCNQ)	Additive	Spin-coating	Al/Si/PEDOT:PSS+ F4TCNQ/Ag	Dark	-	13.23%	35
CuI	Coating	Vacuum deposition	InGa/Si/SiO_X/PEDOT :PSS/Ag/CuI	Dark	Enhanced stability in the air	14.30%	24
GO	Coating	Spin-coating	InGa/Si/PEDOT:PSS/ GO/Ag	Dark	Enhanced stability in the air	13.76%	25
MoO_3	Additive	Spin-coating	Al/PCBM/Si/PEDOT: PSS+MoO_3/Ag	Multi-color	-	13.23%	6

For planar PEDOT:PSS/Si HSCs, there have been many reports that some materials were served as the additive or coating to meet researcher' requirements, such as high PCE, color tunability, excellent stability. Here, we have been summarized representative research in Table 3. It can be seen that only DT can be served as both the additive and coating, while meeting demands of improving PCE, adjusting color, and enhancing stability, especially anti-ultraviolet capability. Moreover, the preparation of efficient, stable and colored devices by using of DT additive and coating has advantages of low cost and simple process, as the simple spin-coating, cheap materials and inexpensive equipments are used during the preparation process.

4. Conclusions

In summary, we have demonstrated an effective approach to not only designing colored PEDOT:PSS/Si HSCs and improving its long-term stability by using a liquid crystal molecule DT coating, but also deliver high-performance devices by adding DT into PEDOT:PSS films. After mixing the DT (1.2 mg mL^{-1}), the experimental results show that the conductivity of PEDOT:PSS films was enhanced due to the change of structure and surface morphology. And then the best PCE of DT-added device was boosted to 13.24% because of less recombination, better junction quality and accelerating charge transport. Notably, when DT coating was covered on the top surface of the DT-added devices, colored devices with 5 colors (purple, blue, cyan, green, yellow) can be achieved. The PCE of them varies from 10.94% (yellow) to 12.36% (purple), exceeding 99% relative PCE of the uncolored control devices. In addition, we have discovered the mechanism about stability damaged by UV radiation, namely UV light can cause the increase of RMS, aggregation of PEDOT chains and disrupted conjugation of PEDOT, leading to a decline in

performance of devices. However, the DT coating covered on the surface of device can effectively avoid the damage from UV irradiation by absorbing UV light and isolating air to obtain an excellent stability of devices. These results reported here offers a practical, economical and convenient method to fabricate efficient, stable and colorful PEDOT:PSS/Si HSCs, and create possibilities of application for colored photovoltaics in Building Integrated Photovoltaic.

Author contributions

Zheng Zhou: Writing - original draft, Investigation. Shibo Chen: Investigation. Yingming Shen: Writing - original draft. Juan Wang: Methodology. Guijun Zhang: Methodology. Yang Shi: Formal analysis. Haixia Wu: Formal analysis. Jingjing Luo: Formal analysis. Xiaohong Cheng: Supervision. Yu Yang: Supervision, Conceptualization.

Conflicts of interest

The authors declare that they have no conflict of interest.

Acknowledgement

This work was supported by the Funds for leading local scientific-technological development by the central government (grant no. 202307AB110010), and the Yunling Scholars Fund of Yunnan Province Xing Dian Talents Program (grant no. KC194317). We also gratefully acknowledge The Advanced Analysis and Measurement Center of Yunnan University.

References

1. B. Q. Sun, M. W. Shao and S. T. Lee, *Advanced Materials*, 2016, **28**, 10539-10547.
2. X. X. Wang, Z. L. Liu, Z. H. Yang, J. He, X. Yang, T. B. Yu, P. Q. Gao and J. C. Ye, *Small*, 2018, **14**, 1704493.
3. K. Ding, X. Zhang, L. Ning, Z. Shao, P. Xiao, A. Ho-Baillie, X. Zhang and J. Jie, *Nano Energy*, 2018, **46**, 257-265.
4. H. Eggers, S. Gharibzadeh, S. Koch, F. Schackmar, D. B. Ritzer, T. Abzieher, B. S. Richards, C. Erban and U. W. Paetzold, *Solar RRL*, 2022, **6**, 2100897.
5. J. H. Noh, S. H. Im, J. H. Heo, T. N. Mandal and S. I. Seok, *Nano Letters*, 2013, **13**, 1764-1769.
6. L.-M. Yu, J.-X. Man, T. Chen, D. Luo, J. Wang, H. Yang, Y.-B. Zhao, H. Wang, Y. Yang and Z.-H. Lu, *Nano Energy*, 2021, **85**, 105937.
7. J. Wang, W. Zhou, Q. Wei, G. Liu, X. Yuan, H. Pen, G. Zhang, R. Wang, C. Wang and Y. Yang, *Advanced Materials Interfaces*, 2023, **10**, 2300187.
8. J. Y. Kim, J. H. Jung, D. E. Lee and J. Joo, *Synthetic Metals*, 2002, **126**, 311-316.
9. J. Ouyang, Q. Xu, C.-W. Chu, Y. Yang, G. Li and J. Shinar, *Polymer*, 2004, **45**, 8443-8450.
10. D. Alemu, H. Y. Wei, K. C. Ho and C. W. Chu, *Energy & Environmental Science*, 2012, **5**, 9662-9671.
11. D.-Y. Khang, *Journal of Physics D: Applied Physics*, 2019, **52**, 503002.
12. Q. Liu, I. Khatri, R. Ishikawa, K. Ueno and H. Shirai, *Applied Physics Letters*, 2013, **102**.
13. X. Fang, T. Song, R. Liu and B. Sun, *The Journal of Physical Chemistry C*, 2014, **118**, 20238-20245.

14. Z. H. Xia, T. Song, J. Sun, S. T. Lee and B. Q. Sun, *Applied Physics Letters*, 2014, **105**, 183503.
15. J. P. Thomas, M. A. Rahman, S. Srivastava, J. S. Kang, D. McGillivray, M. Abd-Ellah, N. F. Heinig and K. T. Leung, *Acs Nano*, 2018, **12**, 9495-9503.
16. Y. H. Kim, C. Sachse, M. L. Machala, C. May, L. Müller-Meskamp and K. Leo, 2011, **21**, 1076-1081.
17. Q. Liu, R. Ishikawa, S. Funada, T. Ohki, K. Ueno and H. Shirai, 2015, **5**, 1500744.
18. S. Jäckle, M. Liebhaber, J. Niederhausen, M. Büchele, R. Félix, R. G. Wilks, M. Bär, K. Lips and S. Christiansen, *ACS Applied Materials & Interfaces*, 2016, **8**, 8841-8848.
19. J. Huang, K. X. Wang, J. J. Chang, Y. Y. Jiang, Q. S. Xiao and Y. Li, *Journal of Materials Chemistry A*, 2017, **5**, 13817-13822.
20. L. Jiang, Z. Zhou, G. J. Zhang, C. G. Li, Q. S. Feng, Q. W. Wei, J. Y. Li, H. X. Wu, Y. Shi, J. Wang and Y. Yang, *Acs Applied Energy Materials*, 2024, **7**, 3927-3936.
21. G. Zhang, H. Peng, Q. Wei, Z. Zhou, H. Wu, J. Luo, J. Wang, X. Wen and Y. Yang, *ACS Omega*, 2024, **9**, 15040-15051.
22. Q. M. Liu, R. Ishikawa, S. Funada, T. Ohki, K. Ueno and H. Shirai, *Advanced Energy Materials*, 2015, **5**, 1500744.
23. J. He, P. Q. Gao, Z. H. Yang, J. Yu, W. Yu, Y. Zhang, J. Sheng, J. C. Ye, J. C. Amine and Y. Cui, *Advanced Materials*, 2017, **29**, 1606321.
24. J. He, P. Gao, Z. Ling, L. Ding, Z. Yang, J. Ye and Y. Cui, *ACS Nano*, 2016, **10**, 11525-11531.
25. M. Lv, Z. Wang, C. Jiao, Y. Zhao, L. Jin, Y. Fu, Q. Liu and D. He, *ACS Applied Energy Materials*, 2021, **4**, 13279-13287.
26. E. Toto, S. Botti, S. Laurenzi and M. Gabriella Santonicola, *Applied Surface Science*, 2020, **513**, 145839.
27. A. Vázquez-López, M. García-Carrión, D. Maestre, S. Z. Karazhanov, E. S. Marstein, B. Méndez and A. Cremades, *Polymer Degradation and Stability*, 2023, **209**, 110272.
28. S. Chen, T. Ma, X. Du, M. Mo, Z. Wang and X. Cheng, *Journal of Molecular Liquids*, 2023, **373**, 121239.
29. X. F. Liao, Q. N. He, G. Q. Zhou, X. X. Xia, P. P. Zhu, Z. Xing, H. M. Zhu, Z. Y. Yao, X. H. Lu and Y. W. Chen, *Chemistry of Materials*, 2021, **33**, 430-440.
30. Q. Lai, R. Zhuang, K. Zhang, T. Wu, L. Xie, R. Zhao, L. Yang, Y. Wang and Y. Hua, *Angew Chem Int Ed Engl*, 2023, **62**, e202305670.
31. Q. Ul Ain, J. X. Xia, H. Kanda, I. R. Alwani, X. X. Gao, H. U. Rehman, G. Shao, V. Jankauskas, K. Rakstys, A. A. Khan and M. K. Nazeeruddin, *Solar Rrl*, 2023, **7**, 2200920.
32. Y. Jiang, B. Luo, F. Jiang, F. Jiang, C. Fuentes-Hernandez, T. Liu, L. Mao, S. Xiong, Z. Li, T. Wang, B. Kippelen and Y. Zhou, *Nano Lett*, 2016, **16**, 7829-7835.
33. J. He, Y. Wan, P. Gao, J. Tang and J. Ye, *Advanced Functional Materials*, 2018, **28**, 1802192.
34. Y. Zhao, L. Zhang, M. Lv, C. Jiao, P. Cheng, Y. Fu, J. Li, Q. Liu and D. He, *ACS Appl Mater Interfaces*, 2021, **13**, 31171-31179.
35. C. Yang, Z. Luo, W. Ma, S. Li, G. Lv, K. Fu, K. Liu, H. Li, H. Sun and X. Chen, *The Journal of Physical Chemistry C*, 2023, **127**, 7974-7986.
36. S. Garreau, J. L. Duvail and G. Louarn, *Synthetic Metals*, 2001, **125**, 325-329.
37. J. Hossain, Q. Liu, T. Miura, K. Kasahara, D. Harada, R. Ishikawa, K. Ueno and H. Shirai, *ACS Appl Mater Interfaces*, 2016, **8**, 31926-31934.
38. Y. Jiang, T. Liu and Y. Zhou, *Advanced Functional Materials*, 2020, **30**, 2006213.
39. Y. J. Xia, K. Sun and J. Y. Ouyang, *Energy & Environmental Science*, 2012, **5**, 5325-5332.
40. Z. Luo, C. Yang, X. Chen, W. Ma, S. Li and K. Fu, *Journal of Materiomics*, 2023, **9**, 438-446.

View Article Online
DOI: 10.1039/D5MA00007F

41. X. Mu, X. Yu, D. Xu, X. Shen, Z. Xia, H. He, H. Zhu, J. Xie, B. Sun and D. Yang, *Nano Energy*, 2015, **16**, 54-61.
42. S. K. Cheung and N. W. Cheung, *Applied Physics Letters*, 1986, **49**, 85-87.
43. C. He, C. M. Zhong, H. B. Wu, R. Q. Yang, W. Yang, F. Huang, G. C. Bazan and Y. Cao, *Journal of Materials Chemistry*, 2010, **20**, 2617-2622.
44. R. K. Sharma, A. Srivastava, P. Kumari, D. Sharma, J. S. Tawale, V. V. Agrawal, B. P. Singh, P. Prathap and S. K. Srivastava, *Surfaces and Interfaces*, 2023, **36**, 102577.
45. H. Yan and H. Okuzaki, *Synthetic Metals*, 2009, **159**, 2225-2228.
46. N. M. Mackie, D. G. Castner and E. R. Fisher, *Langmuir*, 1998, **14**, 1227-1235.
47. X. Crispin, S. Marciniak, W. Osikowicz, G. Zotti, A. W. D. Van der Gon, F. Louwet, M. Fahlman, L. Groenendaal, F. De Schryver and W. R. Salaneck, *Journal of Polymer Science Part B-Polymer Physics*, 2003, **41**, 2561-2583.
48. S. Kondratenko, V. Lysenko, Y. V. Gomeniuk, O. Kondratenko, Y. Kozyrev, O. Selyshchev, V. Dzhagan and D. R. T. Zahn, *Acs Applied Energy Materials*, 2019, **2**, 5983-5991.

View Article Online
DOI: 10.1039/D5MA00007F

Data availability

The data supporting this article have been included as part of the Supplementary Information.